HHS Public Access

Author manuscript

J Biomed Mater Res A. Author manuscript; available in PMC 2017 August 01.

Published in final edited form as:

J Biomed Mater Res A. 2016 August ; 104(8): 2099–2107. doi:10.1002/jbm.a.35735.

Scaffold-mediated BMP-2 minicircle DNA delivery accelerated bone repair in a mouse critical-size calvarial defect model

Michael Keeney[1,2,*], **Michael T. Chung**[3,*], **Elizabeth R. Zielins**[3], **Kevin J. Paik**[3], **Adrian McArdle**[3], **Shane D. Morrison**[3], **Ryan C. Ransom**[3], **Namrata Barbhaiya**[1,2], **David Atashroo**[3], **Gunilla Jacobson**[4], **Richard N. Zare**[4], **Michael T. Longaker**[3], **Derrick C. Wan**[3,*], and **Fan Yang**[1,2,*]

[1]Department of Orthopaedic Surgery, Stanford University School of Medicine, Clark Center E-150, 300 Pasteur Drive, Edwards R105, MC5341, Stanford, California 94305

[2]Department of Bioengineering, Stanford University School of Medicine, Clark Center E-150, 300 Pasteur Drive, Edwards R105, MC5341, Stanford, California 94305

[3]Department of Surgery, Plastic and Reconstructive Surgery Division, Hagey Laboratory for Pediatric Regenerative Medicine, Stanford University School of Medicine, 257 Campus Drive, Stanford University, Stanford, California 94305-5148

[4]Department of Chemistry, Stanford University, 333 Campus Drive Mudd Building, Room 121 Stanford, Stanford, California 94305-4401

Abstract

Scaffold-mediated gene delivery holds great promise for tissue regeneration. However, previous attempts to induce bone regeneration using scaffold-mediated non-viral gene delivery rarely resulted in satisfactory healing. We report a novel platform with sustained release of minicircle DNA (MC) from PLGA scaffolds to accelerate bone repair. MC was encapsulated inside PLGA scaffolds using supercritical CO_2, which showed prolonged release of MC. Skull-derived osteoblasts transfected with BMP-2 MC *in vitro* result in higher osteocalcin gene expression and mineralized bone formation. When implanted in a critical-size mouse calvarial defect, scaffolds containing luciferase MC lead to robust *in situ* protein production up to at least 60 days. Scaffold-mediated BMP-2 MC delivery leads to substantially accelerated bone repair as early as two weeks, which continues to progress over 12 weeks. This platform represents an efficient, long-term nonviral gene delivery system, and may be applicable for enhancing repair of a broad range of tissues types.

Keywords

scaffold; bone regeneration; minicircle; BMP2

Correspondence to: D. C. Wan; dwan@stanford.edu or F. Yang; fanyang@stanford.edu.
*These authors contributed equally to this manuscript

Additional Supporting Information may be found in the online version of this article.

INTRODUCTION

Gene therapy has broad applications including the treatment of genetic disorders, cancer, controlling tissue regeneration, and vaccine delivery. The application of gene therapy in regenerative medicine has been the topic of extensive research over the past decade. The ability to "turn on" or "turn off" target genetic signals during the wound healing process can be exploited to tailor the regenerative response. Non-viral gene therapy using plasmid alone or polyplexes may provide a safer alternative to viral-based gene therapy, and has shown promise for treating various conditions such as diabetic wound healing and promoting angiogenesis.[1–3] Furthermore, DNA cargo can be encapsulated in three-dimensional (3D) scaffolds for prolonged release over time, which allows *in situ* gene delivery in a sustained and spatially controlled manner.

Despite the promise of scaffold-mediated gene delivery for tissue repair, treating bony defects using non-viral gene delivery has proven to be a great challenge. Scaffolds containing DNA encoding bone morphogenetic protein-2 (BMP-2) have been shown to be ineffective in inducing bone formation, even with the addition of mesenchymal stem cells.[4] Similarly, rat calvarial defects treated with Poly(D,L-lactic-*co*-glycolic acid) (PLGA) scaffolds containing BMP-4 DNA resulted in minimal healing (<5%).[5] Even dual plasmid delivery (caALK6+Runx2) to a mouse calvarial defect only resulted in a thin layer of bone along the base of the implant.[6] Bone formation has been shown in a critical-size beagle tibia defect model following treatment with a human parathyroid hormone plasmid entrapped in a polymer matrix sponge. However, a high dose of DNA (100 mg per defect) was required to achieve such bone regeneration, which may lead to undesirable side effects.[7]

To further enhance the gene delivery efficiency, sonoporation, and electroporation techniques have been explored,[8,9] yet the efficacy of bone formation remained unsatisfactory. Bone healing has been achieved using viral-based gene therapy,[9,10] suggesting inefficiency of gene delivery as one of the major obstacles for nonviral-based gene therapy. Recent studies have shown that DNA plasmid transfection efficiency may be limited by formation of repressive heterochromatin from the bacterial cassette: inside the cell, the bacterial cassette sequence is able to covalently bond to the transgene; given the lack of sites for mammalian transcriptional activity, heterochromatin formation begins on the bacterial cassette, subsequently spreading *in cis* to the transgene and silencing it.[11] Chen et al. observed use of minicircle (MC) DNA, produced via excision of the bacterial cassette, resulted in 10–100 fold increased *in vitro* transgene expression.[12,13] *In vivo* transfection data have also shown that efficient expression can be achieved when the bacterial cassette is removed.[14]

Another contributing factor for reduced efficiency of nonviral gene therapy is the lack of effective, controlled delivery for releasing DNA *in situ*. Prolonged delivery of plasmid DNA can enhance protein expression due to increased resident time of the functional plasmid DNA.[15] While a variety of methods exist for controlled release of plasmid DNA, few techniques have achieved long-term delivery, primarily due to detrimental effects of the fabrication process for biodegradable scaffolds on the encapsulated DNA.[16,17] To overcome such issues, supercritical CO_2 has been investigated as an alternative solvent, which is safer

than its organic counterparts, reusable, and enables the encapsulation of plasmid DNA within 3D scaffolds.[18,19] As plasmid DNA can be encapsulated within the polymer matrix, prolonged release can be potentially achieved over several months.[18]

The goal of this study was to develop a scaffold-mediated gene delivery platform that allowed prolonged release of MC DNA *in situ,* and to validate its efficacy in enhancing bone repair using a critical-size mouse calvarial defect model (Fig. 1). We hypothesize that the use of MC DNA and scaffold-mediated prolonged gene delivery will lead to accelerated bone formation. Using supercritical CO_2 as a solvent, we demonstrated MC DNA can be encapsulated within PLGA based scaffolds. PLGA has a long history of use as a biomaterial for bone tissue engineering, particularly in our own laboratory.[24,25] We then characterized the release kinetics of MC DNA from 3D PLGA scaffolds *in vitro* and determined the efficacy on *in vivo* transfection using bioluminescence imaging. Finally, the efficacy of scaffold-mediated delivery of MC DNA encoding BMP-2 for bone repair was examined in a critical-size rodent calvarial defect model, and outcomes were analyzed using micro-computed tomography (micro-CT) imaging and histology. To the author's knowledge, this is the first study to report controlled delivery of MC DNA and the first study to use MC DNA as a treatment for bone regeneration.

EXPERIMENTAL SECTION

Isolation and culture of osteoblasts

CD-1 nude mice (Crl:CD1-*Foxn1*^{nu}) were purchased from Charles River Laboratories (Wilmington, MA) and mesoderm-derived parietal osteoblasts were harvested from skulls of 30-day-old mice, as previously described.[20,21] Briefly, the periosteum and dura mater were carefully stripped from the skull. The peripheral suture complexes of each parietal bone were also carefully removed. Skulls were minced into small chips <1 mm before digestion. Bone chips were digested with 0.2% Dispase II and 0.1% Collagenase A (Roche Diagnostics, Indianapolis, IN) in serum-free medium. The digestion was carried out six times, each for 10 minutes. The first two digestions were discarded and the later four digestions were pooled together. All digestions were neutralized with an equal volume of α-MEM supplemented with 10% fetal calf serum (FCS; Gemini Bioproducts, Woodland, CA), 100 IU/mL penicillin, and streptomycin (Invitrogen, Carlsbad, CA), pelleted, and then resuspended in growth medium. Osteoblasts were plated in 100 mm tissue culture dishes and incubated at 37°C. The medium was changed every other day. Only passage 1 and 2 osteoblasts were used for MC transfection.

Plasmid construction

pMC A2-minicircle backbone vector was obtained from the laboratory of Dr. Joseph Wu (Stanford University). Briefly, this vector contains a multiple cloning site, poly-A tail flanked by attP and attB sites for PhiC31-integrase recombination, 32x Sce-I sites for bacterial backbone degradation, and a kanamycin resistance cassette. Human Ubiquitin C (hUbC) promoter was amplified with primers that added 5′-PstI and 3′-NheI sites. Each of the following inserts was amplified with 5′-NheI and 3′-BamHI sites: GFP was amplified from pCDH_EF1 vector (gift from Dr. Irving Weissman, Stanford University), luciferase

was amplified from pgl3bas vector (Promega, Madison, WI), and human BMP-2 was amplified from pCMV6-XL4 (Origene, Rockville, MD). Primers for amplification are shown in Supporting Information Table S1. Single-step ligation with High-Concentration T4 DNA Ligase (Invitrogen) allowed for the addition of both hUbC, and either BMP-2, GFP, or luciferase. Restriction enzyme digests and DNA sequencing (Pan Facility, Stanford University) confirmed correct promoter and gene insertion.

DH5α sub-cloning efficiency cells (Invitrogen) were used to produce parental plasmid stocks of pMC_hUbC_hBMP-2, pMC_hUbC_GFP, and pMC_hUbC_luciferase. ZYCY10P3S2T *E. coli* cells were obtained from the laboratory of Dr. Joseph Wu and the parental plasmid stocks were transformed into these cells to produce the corresponding MC. Briefly, following overnight culture growth in Terrific Broth (Invitrogen) and 50 μg/mL kanamycin, MC induction media consisting of Luria-Bertani broth (MP Biomedicals, Santa Ana, CA), 0.04N NaOH, and 0.01% L-arabinose (Sigma Aldrich, St. Louis, MO) was added to double the culture volume. The MC was purified using HiSpeed GigaPrep kits (Qiagen, Valencia, CA) and verified on a 1.5% agarose gel relative to the corresponding parental vector.

In vitro transfection and osteogenic differentiation

Osteoblasts were plated in 6-well plates (1×10^5/well). Transfections were performed using SuperFect® (Qiagen), after optimization of the ratio of DNA to transfection agent as per manufacturer's instructions. Upon sub-confluence, cells were incubated with osteogenic differentiation medium (ODM), composed of α-MEM supplemented with 10 μ*M* glycerol β-phosphate, 0.25 μ*M* ascorbic acid (Sigma Aldrich), 10% FCS, and 1% penicillin/streptomycin. The medium was changed every other day. Mineralization of the extracellular matrix was assessed by Alizarin Red staining at day 14 of differentiation, followed by its quantification, by Image J analysis, as previously described.[19]

Reverse transcription and quantitative real timepolymerase chain reaction

RNA from cultivated cells was phase separated using TRIzol® reagent (Invitrogen) and isolated with the RNeasy Mini Kit (Qiagen) according to the manufacturer's protocol. Reverse transcription was performed and osteogenic gene expression was examined by quantitative real-time PCR (qRT-PCR) using the Applied Biosystems Prism 7900HT sequence detection system (Applied Biosystems, Foster City, CA) and Power SYBR Green PCR Master Mix (Applied Biosystems). Target quantities were obtained and then normalized to endogenous GAPDH levels. Normalized target values were then calibrated to expression of GFP transfected cells at day 0 to generate relative expression levels. Primers for genes examined were created from PrimerBank (Supporting Information Table S1).[20]

Protein isolation and western blot analysis

Osteoblasts were collected at day 7 of osteogenic differentiation. Cells were lysed with cold RIPA buffer composed of 50 mmol/L of pH 7.5 HEPES, 150 mmol/L of NaCl, 1 mmol of EDTA, 10% glycerol, 1% Triton-X-100, 25 m*M* sodium fluoride, 1 m*M* sodium orthovanadate, and Protease Inhibitor Cocktail (Sigma Aldrich). Cell lysates (40 μg) were electrophoresed on a 12% NuPAGE® Bis-Tris precast gel (Novex) and transferred to a

PVDF membrane, which was blocked in 5% non-fat milk for one hour. Membranes were incubated overnight at 4°C with a primary rabbit anti-mouse BMP-2 antibody (1:1000 dilution) (Abcam, Cambridge, MA). A secondary horseradish-peroxidase conjugated antibody (Cell Signaling, Danvers, MA) at a 1:2000 dilution was used for detection with ECL Plus (Amersham, Waukesha, WI). Quantification of bands was performed using ImageJ (NIH, Bethesda, MD). Quantified bands were normalized to betaactin loading control and presented as a ratio relative to the GFP MC group.

Scaffold fabrication

Ester terminated poly(DL-lactide-*co*-glycolide) (PLGA) (85/15, inherent viscosity 0.55−0.75 dL/g Lactel Absorbable Polymers, Birmingham, AL) (70 mg) was ground into fine particles (approximately 500 μm in diameter) and combined with 100 μL MC (BMP-2, GFP, or luciferase; 16.1 mg/mL) suspended in elution buffer (Buffer EB, Qiagen). The solution was placed into a Teflon mold and lyophilized for 24 h. Following lyophilization, the mold was placed in a sealed chamber connected to a CO_2 supply. CO_2 was injected into the chamber with temperature set at 35°C until the pressure reached 12.4 MPa. At this temperature and pressure, CO_2 becomes a supercritical fluid and acts as a plasticizer for PLGA. Following a 1-h incubation period, the seal was removed and pressure was allowed equilibrate to atmospheric conditions over a period of seven minutes by opening a pressure release valve. As CO_2 reverted back to a gaseous state, the PLGA began to foam, resulting in pore formation and encapsulation of MC within the scaffold. A skin is formed on the outer surface of the PLGA, which was subsequently removed using a scalpel blade. Implants were cut out using a 4 mm skin biopsy (Miltex, Plainsboro, NJ) to produce final scaffolds measuring 4 mm in diameter and 0.6 mm thick. Each scaffold was designed to contain 90 μg MC.

Scanning electron microscopy

Scanning electron microscope (SEM) imaging was performed to visualize the porous structure of scaffolds produced using supercritical CO_2. Scaffolds were sectioned using a scalpel blade, sputter coated and imaged with an SEM (3400N VP-SEM, Hitachi, Dallas, TX).

Minicircle release assay

To quantify the rate of MC release *in vitro*, implants (as described above) were placed in 200 μl PBS (Gibco) and maintained in a humid atmosphere at 37°C. At specified time points, the supernatant was removed and replenished with new PBS. The supernatant was stored at −20°C until time of assay. MC concentration in the supernatant was quantified using a PicoGreen® assay (Invitrogen). Briefly, 50 μL of supernatant was combined with 50 μL of PBS followed by the addition of 100 μL PicoGreen® dye prepared according to the manufacturer's protocol. MC of a known concentration was used to form a standard curve from which MC concentration in the supernatant could be determined. The resulting fluorescence was measured using a plate reader (Spectramax M2e, Molecular Devices, Sunnyvale, CA) with an excitation/emission set to 480/520 nm.

In vivo implantation

All experiments were performed in accordance with the Stanford University Animal Care and Use Committee Guidelines and approved APLAC protocols. For evaluation of *in vivo* osteogenesis, nonhealing, critical-size (4 mm) calvarial defects were created in the right parietal bone of adult (60-day-old) female CD-1 nude mice, as previously described.[21] Implants, as described above, containing MC encoding for BMP-2, luciferase, or GFP were placed into the defect space (n=3 per group). For micro-CT scans, the mice were anesthetized with 2–3% inhaled isoflurane. Imaging was performed using a Siemens Inveon MicroPET/CT scanner (Siemens Medical Solutions Inc., Malvern, PA). Using our scan protocol parameters, each high resolution 100 μm image was acquired in a total scan time of 10 min. Mice were immediately scanned postoperatively and then at 2-, 4-, 6-, 8-, and 12-weeks following surgery. Data were reconstructed into 3D surfaces using Inveon Research Workplace 4.0 (Siemens Medical Solutions Inc.). The 3D reconstructed images were then analyzed using ImageJ by quantifying pixels in the defect. Percentage healing was determined by dividing the area of regenerated bone by the baseline defect size.

Bioluminescence imaging

Bioluminescence Imaging (BLI) imaging was performed on the same animals at indicated time points for 60 days. Animals were anesthetized by 2–3% inhaled isoflurane and injected intraperitoneally with D-Luciferin (Sigma-Aldrich) at 100 mg/kg body weight. An IVIS Spectrum (Xenogen, Hopkinton, MA) was used to image animals. Each animal was scanned until the peak total flux signal was reached, then radiance was recorded from regions of interest. Radiance was quantified in photons per second per centimeter squared per steradian.

Histological analysis

At 12 weeks postoperatively, calvariae were harvested, immediately fixed in 10% formalin overnight, decalcified in 19% EDTA, dehydrated through an ethanol series, and embedded in paraffin, as previously described.[22] Deparaffinized sections were stained with Movat's Pentachrome and Aniline Blue to detect bone matrix formation. Bright-field images were obtained with a 5X or 200X objective at room temperature using a Leica DM5000 microscope (Leica Microsystems Inc., Wetzlar, Germany) equipped with a DFC300FX camera. The images were analyzed using Leica IM1000 Version 4.0 Image Acquisition Software (Leica Microsystems).

Statistical analysis

In figures, bar graphs represent means, and error bars represent one standard deviation. Unless otherwise stated, statistical analysis was performed using a one-way analysis of variance (ANOVA) for multiple group comparisons and a two-tailed Student's t test was used to directly compare two groups. A value of $*p<0.05$ was considered significant. All data are presented as mean±standard deviation.

RESULTS

BMP-2 MC enhances BMP-2 expression and bone formation *in vitro*

We first examined the effects of BMP-2 MC transfection on osteoblasts *in vitro* using GFP- or BMP-2 encoding MC DNA. As seen in Figure 2(a), osteoblasts transfected with Super-Fect® demonstrated GFP production under fluorescence microscopy. Osteoblasts were subsequently transfected in similar fashion using BMP-2 MC. Protein was then collected from osteoblasts at day 7 of osteogenic differentiation. As expected, un-transfected osteoblasts underwent differentiation as cells were cultured in ODM, however differentiation was enhanced in the BMP-2 transfected group as demonstrated by increased gene expression and protein and matrix synthesis. Western blot analysis demonstrated a significantly higher amount of BMP-2 protein present in osteoblasts transfected with BMP-2 MC than in osteoblasts transfected with GFP MC (**$p<0.01$) [Fig. 2(b)]. RNA was collected from osteoblasts at Days 0, 7, and 14. Transcriptional analysis also revealed higher levels of BMP-2 expression in cells transfected with BMP-2 MC, with the most prominent difference occurring at day 0 (***$p<0.001$) [Fig. 2(c)]. Osteocalcin, a mature bone marker implicated in bone mineralization, was also significantly increased in BMP-2 MC transfected cells across all time points (day 0 **$p<0.01$, day 7 **$p<0.01$, and day 14 *$p<0.05$) [Fig. 2(d)]. Cells transfected with BMP-2 MC also qualitatively exhibited greater Alizarin Red staining after 14 days of osteogenic differentiation treatment than cells transfected with the control GFP MC [Fig. 2(e–g)]. Quantification of staining using ImageJ confirmed this finding (*$p<0.05$) [Fig. 2(g)].

Scaffold fabrication and minicircle release

Scanning electron microscopy was performed to evaluate scaffolds produced at 12.4 MPa and 35°C. Cross-sectional images of final scaffolds demonstrated an interconnected structure with pore size around 200 μm in diameter [Fig. 3(a)]. Scaffolds containing MC demonstrated a smoother surface with slightly decreased macroporosity due to MC DNA filling [Fig. 3(b)]. Release of MCs from the PLGA scaffold was then evaluated at 37°C. Over the first week, 30% of the total embedded MCs were released, followed by a gradual release over 60 days, by which time 50% of total encapsulated DNA was released [Fig. 3(c)]. As the PLGA remained intact after eight weeks *in vitro*, the remaining MCs were likely trapped within the polymer structure and would be released upon scaffold degradation.

Luciferase is up-regulated for 60 days *in vivo*

To evaluate *in vivo* release and local uptake of MCs, a calvarial defect was created in the right parietal bone of mice. Scaffolds containing MC encoding for luciferase were placed into these defects. Bioluminescence imaging was then performed over 60 days to monitor luciferase protein production as a result of MC transfection. Over the first week following implantation, we noted high luciferase production followed by sustained protein production at lower levels over the following seven weeks [Fig. 4(a)]. Furthermore, bioluminescent images obtained on day 60 show localization of signal to the region of scaffold implantation indicating that transfection and luciferase protein production remained localized [Fig. 4(b)].

Sustained *in vivo* bone formation occurred over 12 weeks

Critical-size calvarial defects were then created in the right parietal bone of mice and scaffolds with MC encoding for BMP-2 or GFP were placed into the defect space. Bone formation was monitored over 12 weeks using micro-CT. Control scaffolds with GFP MC did not induce bone formation, indicating that supercritical PLGA scaffolds alone are not sufficient for inducing endogenous bone repair [Fig. 5(a)]. However, scaffolds containing MC encoding for BMP-2 show enhanced bone formation over the 12-week period *in vivo* [Fig. 5(b)]. The most significant period of bone formation occurred over the first 2 weeks, with 23% healing noted in BMP-2 MC treated defects compared to control defects, which remained at 0% (***$p<0.001$) [Fig. 5(c)]. At the time of sacrifice (12 weeks), 57% bone healing had occurred in BMP-2 MC treated defects, while signs of bone regeneration were not observed in control scaffolds with GFP MC (****$p<0.0001$).

Histological analysis confirms robust bone formation

Calvariae were harvested at week 12 and histological assessment of the two groups was performed. Staining for collagen fibers with Aniline Blue, minimal tissue formation was noted across defects treated with GFP MC scaffolds [Fig. 6(a,b)]. In contrast, tissue regeneration spanning the entire defect was noted with BMP-2 MC scaffolds [Fig. 6(c,d)]. Quantification of Aniline Blue stained histological images confirmed significantly increased tissue formation in the BMP-2 MC group (***$p<0.001$) [Fig. 6(e)]. Similarly, staining specifically for bone using Movat's Pentachrome showed robust bone regeneration with good osteointegration in the BMP-2 MC cohort (Supporting Information Fig. S1). In contrast, the control group with GFP MC failed to form bone.

DISCUSSION

While viral-based gene therapy has shown promising efficacy in bone repair, applying nonviral based gene delivery to promote bone regeneration has proven difficult to achieve. This is likely caused by low transfection efficacy using conventional plasmid DNA, and the lack of delivery platforms for sustained *in situ* delivery of DNA. To enhance the gene delivery efficiency, we have chosen to use MC DNA, which does not contain the bacterial plasmid backbone. To achieve prolonged MC DNA *in situ*, we encapsulated MC DNA within PLGA scaffolds using supercritical CO_2, which allows fabrication of DNA-containing, macroporous scaffolds without the use of organic solvents. The results of our release kinetics show prolonged release *in vitro* of MC DNA over 60 days. Upon implantation into a mouse critical-size calvarial defect model, MC was released to transfect cells in the local environment, and this resulted in transgenic protein expression up to 60 days after initial placement. Finally, delivery of MC encoding for BMP-2 resulted in a marked increase in bone formation within the defect over a 12-week period.

In the current study, we have chosen to encapsulate MC DNA within PLGA scaffolds using supercritical CO_2 to best retain the biological activity of the loaded genes. CO_2 reaches a supercritical state at 7.38 MPa and 31.1°C.[23] Under these conditions, CO_2 has a gas-like diffusivity and a liquid-like density. Due to the gaseous-like property of supercritical CO_2, it penetrates PLGA and plasticize the polymer. When the pressure is subsequently released,

nucleation sites occur within the polymer matrix as supercritical CO_2 returns to a gas state; hence, bubbles form to produce pores within the polymer matrix.[24] Pore size and density can be controlled by pressure, temperature, soaking time, and pressure release rate, thereby allowing MC encapsulation within PLGA and pore formation to occur in a single step process. High pressure CO_2 (5.5 MPa) has also been used to encapsulate DNA within PLGA. However, this technique requires the use of porogens to form the porous network.[25,26] Prolonged exposure to high pressure CO_2 (5.5 MPa for 16 hours) has a similar effect to supercritical CO_2, whereby CO_2 infiltrates the polymer and upon return to atmospheric pressure, causes swelling and fusion of PLGA particles. The high-pressure approach is slower and does not allow control over scaffold structure, thus requiring a porogen to artificially create the porous network. Removal of the porogen prior to use, though, can incur DNA losses of 50–60%.[27]

One important consideration for developing a scaffold-mediated gene delivery platform is the tunability of release kinetics to suit different applications. In our system, the rate at which plasmid is released may be controlled by varying the inherent viscosity (i.v.) of PLGA. It has been demonstrated that PLGA 75:25 with i.v. of 0.2 and 0.7 results in total plasmid release over 15 days and approximately 60 days respectively.[27] As a direct relationship exists between i.v. and molecular weight of PLGA (that is, increasing molecular weight also increases i.v.), higher molecular weight polymers are more suited for sustained release of plasmid DNA. The reason for this phenomenon is likely due to the ability of higher molecular weight (higher i.v.) polymers to flow under supercritical CO_2 conditions and encapsulate DNA within the polymer matrix. PLGA used in the current study contains an i.v. of 0.55 – 0.75 which, according to previous reports, is in a range suitable for sustained DNA delivery.[27]

One challenge for designing an effective controlled drug delivery system is to avoid burst release during the early phase. For example, previous research showed that scaffolds fabricated using high-pressure CO_2 (5.5 MPa) resulted in over 90% DNA release over the first week (PLGA 85:15).[27] Our results demonstrated a slower release profile using supercritical CO_2 in place of high pressure CO_2, with 50% of total MC released after 60 days. A bi-phasic release profile was observed where 30% was released over the first seven days followed by a sustained delivery period. Such bi-phasic release profiles may be desirable for tissue regeneration whereby an initial high concentration of biomolecules will stimulate the healing process followed by a slower rate of delivery for guiding continuous tissue regeneration.[28] Depending on the rate of wound healing, release characteristics may need to be optimized. In the current study, with gradual formation of osteoid, prolonged delivery of MC contributed to the enhanced ultimate bone regeneration noted.

To enhance the efficacy of transfection, the design of the plasmid itself may also be optimized. Previous scaffold-mediated gene delivery platforms have used conventional plasmid design that includes the bacterial backbone. We have chosen to use MC DNA in the present study, which did not contain the bacterial cassette. As the bacterial cassette may contribute to gene silencing, its removal resulted in a smaller plasmid with increased transfection efficiency.[11,12] It has also been suggested that MCs may have increased uptake through the nuclear pore membrane by decreasing plasmid size.[29] Our *in vitro* data showed

effective MC DNA delivery, and that BMP-2 overexpression led to enhanced osteocalcin expression and mineralization. The initial high expression of BMP-2 decreased by day 7, although the level remained 50-fold higher than GFP transfected cells. (Data not shown) It should be noted that *in vitro* studies require the use of a transfection agent, however naked DNA has the ability to transfect without a carrier *in vivo*;[30,31] SuperFect® was used to achieve *in vitro* transfection in the current study. The differences between *in vitro* and *in vivo* transfection capabilities are poorly understood.

For *in vivo* experiments, we have chosen to release naked MC DNA rather than complexed DNA. While others have shown scaffolds containing complexed plasmid DNA to be effective at bone healing,[32] our pilot studies found that complexed MC DNA released from scaffolds lost its functionality within 72 hours *in vitro* and failed to transfect *in vivo* (data not shown). The reason for loss of function was likely hydrolysis of the polymer (when using short backbones) and inability to release MC-DNA. To evaluate the efficacy of released MC DNA to transfect endogenous cells *in vivo*, we implanted scaffolds containing luciferase MC DNA, and monitored the luciferase protein production *in situ* over time using bioluminescence imaging. Our results confirmed sustained luciferase protein production in the cranial defect site, and the protein production profile observed *in vivo* mirrored our *in vitro* release kinetics. An initial high concentration of MC over the first seven days resulted in elevated protein production at earlier time points *in vivo*, which translated to rapid bone formation upon delivery of MC encoding for BMP-2.

Scaffold-mediated BMP-2 MC delivery led to intense collagen deposition with centrally located nuclei, indicating mature woven bone formation. In contrast, defects treated with scaffold containing GFP MC only showed a thin, fibrous collagenous tissue. The centrally located nuclei were surrounded by ground substance (blue/green stain), indicating the formation of Haversian canals. Although PLGA may induce inflammation and cytotoxicity due to the acidic products of degradation,[33] we observed direct bone-implant apposition with no signs of excessive inflammation. The low level of inflammation may be explained by our choice of PLGA 85:15, which degrades slower than PLGA 50:50, therefore helping prevent the accumulation of acid by-products.

Our results also showed substantially enhanced bone repair compared to the efficacy reported by previous studies. For example, BMP-4 DNA delivery from PLGA scaffolds formed using high-pressure CO_2 only produced 4% bone formation in rat calvarial defects after 15 weeks.[5] Complexing plasmid DNA with a cationic polymer increased bone formation, but only to a maximum of approximately 17% at Week 15.[5] In contrast, we demonstrated that sustained delivery of MC DNA led to accelerated bone formation, with over 57% bone void filled with mineralized bone tissues by 12 weeks. One additional advantage of our platform is the need for less DNA plasmid to achieve efficient bone formation. In our study, only 1.6 mg DNA was used per defect, which is almost two orders of magnitude lower compared to previous studies.[7] BMP-2 can act as a chemotactic, mitogenic, and differentiation agent in bone formation.[34] Although local delivery of recombinant BMP-2 protein can stimulate accelerated bone formation, it requires use of supraphysiological concentration of proteins and may lead to undesirable excessive bone formation.[35] In contrast, our platform engages in endogenous cells to produce BMP-2 *in*

situ, which may decrease risks of undesirable side effects associated with direct protein delivery.

CONCLUSION

In summary, here we report the development of a PLGA-based scaffold containing MC DNA using a supercritical CO_2 method, which allows sustained delivery of MC over at least two months both *in vitro* and *in vivo*. PLGA scaffolds containing MC DNA were fabricated in a one-step process using supercritical CO_2, which removes the need to use organic solvents hence preserving biological activity of the encapsulated cargo. We further demonstrated that scaffold-mediated release of BMP-2 MC DNA *in situ* led to robust and accelerated bone repair in a critical-size calvarial defect model, as shown by micro-CT imaging and histology. Our results show that scaffold-mediated delivery of MC DNA represent a promising platform for enhancing bone repair *in vivo*, and such platforms may be broadly useful for treating long bone defects or regenerating other tissue types as well.

Acknowledgments

Contract grant sponsor: National Institute of Health; contract grant number: NIHR21DE019274, NIHR01DE019434, NIHR01DE021683, NIHU01HL099776

Contract grant sponsors: Basil O'Connor Starter Scholar Research Award from March of Dimes Foundation (FY), Stanford Bio-X Interdisciplinary Initiative Program grant (FY), the Stanford Child Health Research Institute grant (FY), the Oak Foundation (MTL), the Hagey Laboratory for Pediatric Regenerative Medicine (MTL), ACS Franklin H. Martin Faculty Research Fellowship, the Hagey Laboratory for Pediatric Regenerative Medicine, and the Stanford University Child Health Research Institute Faculty Scholar Award.

The authors would like to thank Cell Sciences Imaging Facility at Stanford for assistance with scanning electron microscopy. The authors would also like to thank Stanford Center for Innovation in In Vivo Imaging for assistance with bioluminescence imaging and micro-CT imaging.

References

1. Kwon MJ, An S, Choi S, Nam K, Jung HS, Yoon CS, Ko JH, Jun HJ, Kim TK, Jung SJ, Park JH, Lee Y, Park JS. Effective healing of diabetic skin wounds by using nonviral gene therapy based on minicircle vascular endothelial growth factor DNA and a cationic dendrimer. J Gene Med. 2012; 14:272–278. [PubMed: 22407991]
2. Shimoda M, Chen S, Noguchi H, Matsumoto S, Grayburn PA. In vivo non-viral gene delivery of human vascular endothelial growth factor improves revascularisation and restoration of euglycaemia after human islet transplantation into mouse liver. Diabetologia. 2010; 53:1669–1679. [PubMed: 20405100]
3. Sunshine J, Green JJ, Mahon KP, Yang F, Eltoukhy AA, Nguyen DN, Langer R, Anderson DG. Small-molecule end-groups of linear polymer determine cell-type gene-delivery efficacy. Adv Mater. 2009; 21:4947–4951. [PubMed: 25165411]
4. Hosseinkhani H, Yamamoto M, Inatsugu Y, Hiraoka Y, Inoue S, Shimokawa H, Tabata Y. Enhanced ectopic bone formation using a combination of plasmid DNA impregnation into 3-D scaffold and bioreactor perfusion culture. Biomaterials. 2006; 27:1387–1398. [PubMed: 16139884]
5. Huang YC, Simmons C, Kaigler D, Rice KG, Mooney DJ. Bone regeneration in a rat cranial defect with delivery of PEI-condensed plasmid DNA encoding for bone morphogenetic protein-4 (BMP-4). Gene Ther. 2005; 12:418–426. [PubMed: 15647766]
6. Itaka K, Ohba S, Miyata K, Kawaguchi H, Nakamura K, Takato T, Chung UI, Kataoka K. Bone regeneration by regulated in vivo gene transfer using biocompatible polyplex nanomicelles. Mol Ther. 2007; 15:1655–1662. [PubMed: 17551504]

7. Bonadio J, Smiley E, Patil P, Goldstein S. Localized, direct plasmid gene delivery in vivo: prolonged therapy results in reproducible tissue regeneration. Nat Med. 1999; 5:753–759. [PubMed: 10395319]
8. Sheyn D, Kimelman-Bleich N, Pelled G, Zilberman Y, Gazit D, Gazit Z. Ultrasound-based nonviral gene delivery induces bone formation in vivo. Gene Ther. 2008; 15:257–266. [PubMed: 18033309]
9. Rose L, Uludag H. Realizing the potential of gene-based molecular therapies in bone repair. Journal of bone and mineral research: the official journal of the American Society for Bone and Mineral Research. 2013; 28:2245–2262.
10. Lieberman JR, Le LQ, Wu L, Finerman GA, Berk A, Witte ON, Stevenson S. Regional gene therapy with a BMP-2-producing murine stromal cell line induces heterotopic and orthotopic bone formation in rodents. J Orthop Res. 1998; 16:330–339. [PubMed: 9671928]
11. Chen ZY, Riu E, He CY, Xu H, Kay MA. Silencing of episomal transgene expression in liver by plasmid bacterial backbone DNA is independent of CpG methylation. Mol Ther. 2008; 16:548–556. [PubMed: 18253155]
12. Chen ZY, He CY, Ehrhardt A, Kay MA. Minicircle DNA vectors devoid of bacterial DNA result in persistent and high-level transgene expression in vivo. Mol Ther. 2003; 8:495–500. [PubMed: 12946323]
13. Darquet AM, Cameron B, Wils P, Scherman D, Crouzet J. A new DNA vehicle for nonviral gene delivery: supercoiled minicircle. Gene Ther. 1997; 4:1341–1349. [PubMed: 9472558]
14. Chang CW, Christensen LV, Lee M, Kim SW. Efficient expression of vascular endothelial growth factor using minicircle DNA for angiogenic gene therapy. Journal of controlled release: official journal of the Controlled Release Society. 2008; 125:155–163. [PubMed: 18063165]
15. Holladay C, Keeney M, Greiser U, Murphy M, O'Brien T, Pandit A. A matrix reservoir for improved control of non-viral gene delivery. Journal of controlled release: official journal of the Controlled Release Society. 2009; 136:220–225. [PubMed: 19233237]
16. Holmberg B, Malmfors T. The cytotoxicity of some organic solvents. Environ Res. 1974; 7:183–192.
17. Li GC, Hahn GM, Shiu EC. Cytotoxicity of commonly used solvents at elevated temperatures. J Cell Physiol. 1977; 93:331–334. [PubMed: 591566]
18. Heyde M, Partridge KA, Howdle SM, Oreffo RO, Garnett MC, Shakesheff KM. Development of a slow non-viral DNA release system from PDLLA scaffolds fabricated using a supercritical CO2 technique. Biotechnol Bioeng. 2007; 98:679–693. [PubMed: 17405179]
19. Tservistas M, Levy MS, Lo-Yim MY, O'Kennedy RD, York P, Humphrey GO, Hoare M. The formation of plasmid DNA loaded pharmaceutical powders using supercritical fluid technology. Biotechnol Bioeng. 2001; 72:12–18. [PubMed: 11084588]
20. Li S, Quarto N, Senarath-Yapa K, Grey N, Bai X, Longaker MT. Enhanced Activation of Canonical Wnt Signaling Confers Mesoderm-Derived Parietal Bone with Similar Osteogenic and Skeletal Healing Capacity to Neural Crest-Derived Frontal Bone. PloS one. 2015; 10:e0138059. [PubMed: 26431534]
21. Li S, Meyer NP, Quarto N, Longaker MT. Integration of multiple signaling regulates through apoptosis the differential osteogenic potential of neural crest-derived and mesoderm-derived Osteoblasts. PloS one. 2013; 8:e58610. [PubMed: 23536803]
22. Kretlow JD, Jin YQ, Liu W, Zhang WJ, Hong TH, Zhou G, Baggett LS, Mikos AG, Cao Y. Donor age and cell passage affects differentiation potential of murine bone marrow-derived stem cells. BMC cell biology. 2008; 9:60. [PubMed: 18957087]
23. Wang X, Seed B. A PCR primer bank for quantitative gene expression analysis. Nucleic acids research. 2003; 31:e154. [PubMed: 14654707]
24. Cowan CM, Shi YY, Aalami OO, Chou YF, Mari C, Thomas R, Quarto N, Contag CH, Wu B, Longaker MT. Adipose-derived adult stromal cells heal critical-size mouse calvarial defects. Nature biotechnology. 2004; 22:560–567.
25. Levi B, James AW, Nelson ER, Vistnes D, Wu B, Lee M, Gupta A, Longaker MT. Human adipose derived stromal cells heal critical size mouse calvarial defects. PloS one. 2010; 5:e11177. [PubMed: 20567510]

26. Saito M. History of supercritical fluid chromatography: instrumental development. Journal of bioscience and bioengineering. 2013; 115:590–599. [PubMed: 23318247]
27. Barry JJ, Silva MM, Popov VK, Shakesheff KM, Howdle SM. Supercritical carbon dioxide: putting the fizz into biomaterials. Philos Trans A Math Phys Eng Sci. 2006; 364:249–261. [PubMed: 17464360]
28. Mooney DJ, Baldwin DF, Suh NP, Vacanti JP, Langer R. Novel approach to fabricate porous sponges of poly(D,L-lactic-co-glycolic acid) without the use of organic solvents. Biomaterials. 1996; 17:1417–1422. [PubMed: 8830969]
29. Jang JH, Rives CB, Shea LD. Plasmid delivery in vivo from porous tissue-engineering scaffolds: transgene expression and cellular transfection. Mol Ther. 2005; 12:475–483. [PubMed: 15950542]
30. Shea LD, Smiley E, Bonadio J, Mooney DJ. DNA delivery from polymer matrices for tissue engineering. Nature Biotechnol. 1999; 17:551–554. [PubMed: 10385318]
31. Silva EA, Mooney DJ. Effects of VEGF temporal and spatial presentation on angiogenesis. Biomaterials. 2010; 31:1235–1241. [PubMed: 19906422]
32. Needham CJ, Shah SR, Dahlin RL, Kinard LA, Lam J, Watson BM, Lu S, Kasper FK, Mikos AG. Osteochondral tissue regeneration through polymeric delivery of DNA encoding for the SOX trio and RUNX2. Acta Biomater. 2014; 10:4103–4112. [PubMed: 24854956]
33. Sung HJ, Meredith C, Johnson C, Galis ZS. The effect of scaffold degradation rate on three-dimensional cell growth and angiogenesis. Biomaterials. 2004; 25:5735–5742. [PubMed: 15147819]
34. Sykaras N, Opperman LA. Bone morphogenetic proteins (BMPs): how do they function and what can they offer the clinician? Journal of oral science. 2003; 45:57–73. [PubMed: 12930129]
35. Wong DA, Kumar A, Jatana S, Ghiselli G, Wong K. Neurologic impairment from ectopic bone in the lumbar canal: a potential complication of off-label PLIF/TLIF use of bone morphogenetic protein-2 (BMP-2). The spine journal: official journal of the North American Spine Society. 2008; 8:1011–1018. [PubMed: 18037352]

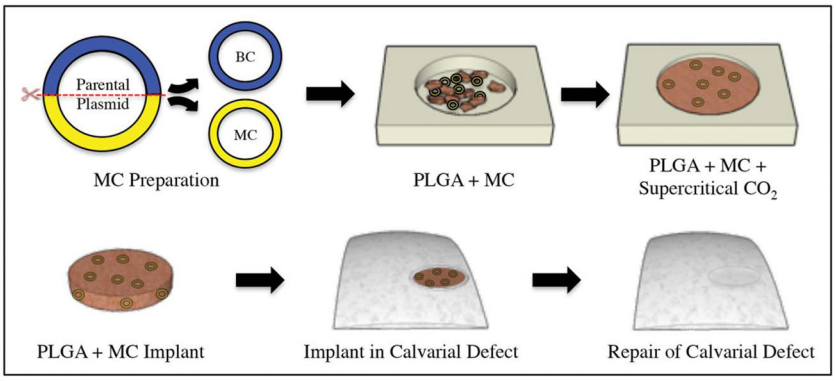

FIGURE 1.

Schematic diagram describing the synthesis of MC-containing PLGA scaffolds, and subsequent use for the repair of calvarial defects in mice. (Top) MC DNA is derived from a parent plasmid by removal of the bacterial cassette (BC). MC DNA is then fused with PLGA under supercritical CO2. (Bottom) Scaffold containing BMP-2 MC DNA is implanted into a mouse critical-size calvarial defect model for bone repair.

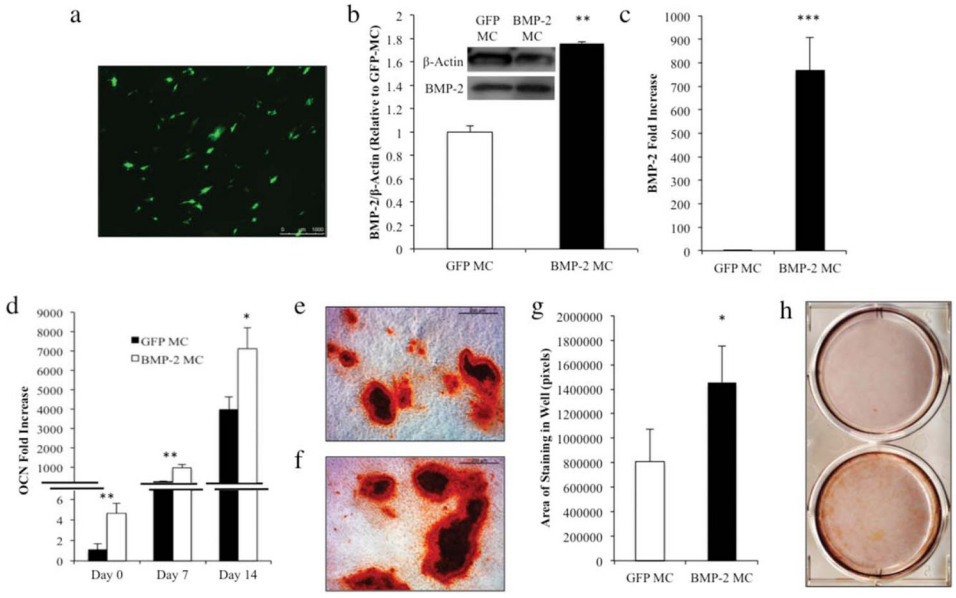

FIGURE 2.

(a) Fluorescent microscope images of osteoblasts two days after transfection with MC encoding for GFP using the same transfection conditions as used for BMP-2. Transfection efficiency approximately 15%, as determined by GFP+ cells per high power field (b) Western blot and quantification of BMP-2 protein expression by osteoblasts transfected with MC encoding for BMP-2 relative to GFP MC (**p<0.01). Data are normalized to β-actin expression. (c, d) qRT-PCR for BMP-2 expression on day 0 (***p<0.001) and osteocalcin expression on day 0 (**p<0.01), day 7 (**p<0.01), and day 14 (*p<0.05) following osteoblast transfection with MC encoding for BMP-2 or GFP. Data are presented as mean ±standard deviation and all data are normalized to GFP MC day 0, with n=3 wells for each group. Bright-field images of Alizarin Red stained osteoblasts 14 days after transfection with MC encoding for (e) GFP or (f) BMP-2. (g) Quantification of Alizarin Red stained osteoblasts (h) demonstrating amount of extracellular mineralization after 14 days *in vitro* (*p<0.05). Data are presented as mean±SD, n=3.

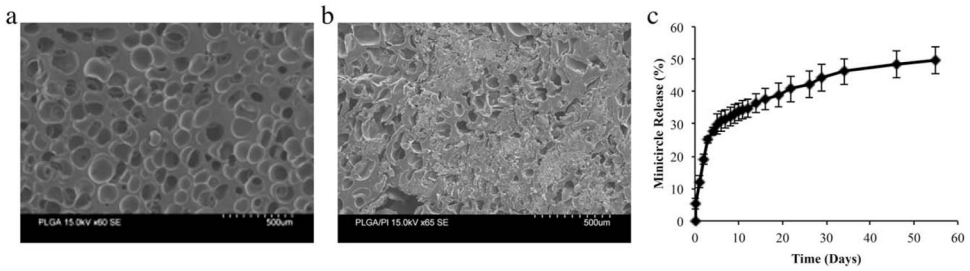

FIGURE 3.

Cross sectional scanning electron microscope images of PLGA scaffolds formed using supercritical CO2 (a) without and (b) with the inclusion of MC. (c) Minicircle release from PLGA scaffold created using supercritical CO2. Release was performed in PBS at 37°C and quantified using PicoGreen®. Data are presented as mean±SD, n=3.

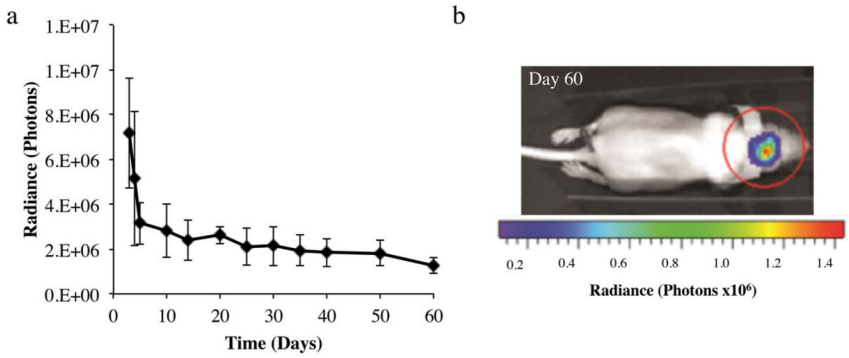

FIGURE 4.

(a) *In vivo* luciferase protein expression as measured by *ex vivo* bioluminescence imaging. Data are presented as mean±standard deviation, n=3. (b) Ex vivo image of mouse implanted with PLGA scaffold containing MC encoding for luciferase. Image was acquired 60 days after implantation.

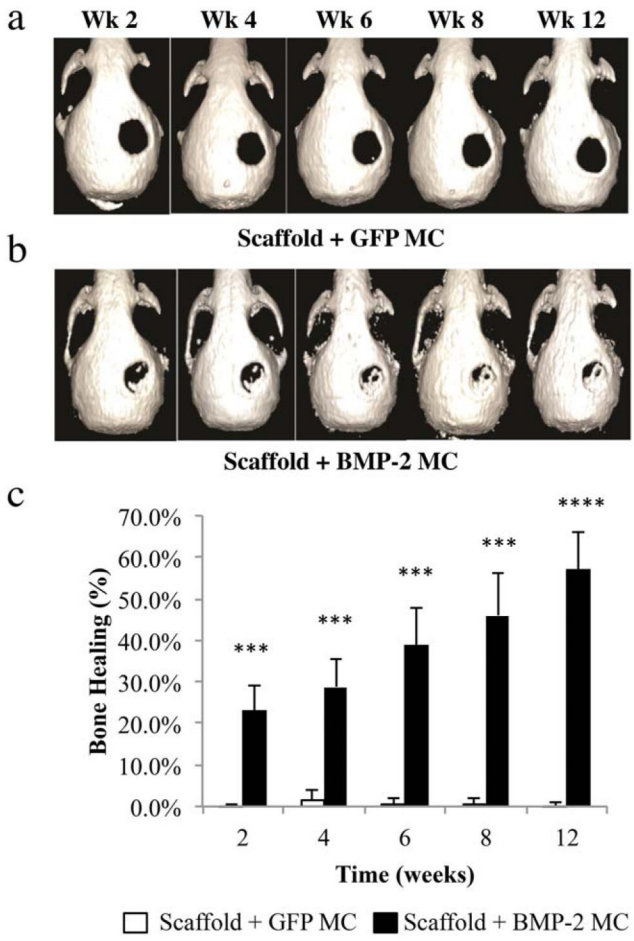

FIGURE 5.

Reconstructed micro-CT images depicting bone regeneration in critical-size defects created in the parietal bone of mice. Defects were treated with PLGA scaffolds containing MC encoding for (a) GFP or (b) BMP-2. (c) Quantitative analysis of reconstructed micro-CT images demonstrating % bone healing at week 2 (***p<0.001), week 4 (***p<0.001), week 6 (***p<0.001), week 8 (***p<0.001), and week 12 (****p<0.0001), as determined by dividing the area of regenerated bone by the defect area on Day 0. Data are presented as mean±SD, n=3.

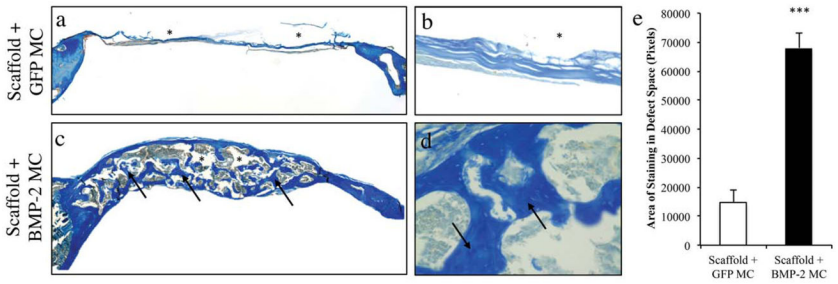

FIGURE 6.

Aniline Blue stained histological images of calvarial defects treated with PLGA containing minicircle encoding for (a, b) GFP and (c, d) BMP-2. Images (a) and (c) were acquired at 5X magnification while images (b) and (d) were acquired at 200X magnification. (*) PLGA scaffold, (Arrows) New bone formation. (e) Quantification of Aniline Blue stained histological images indicating amount of osteoid in the defect area (***p<0.001). Data are presented as mean±SD, n=3.